Nanoscale

Accepted Manuscript

This article can be cited before page numbers have been issued, to do this please use: J. C. C. Azcárate, S. Diaz, J. Fauerbach, F. Gillanders, A. Rubert, E. Jares-Erijman, T. M. Jovin and M. H. H. Fonticelli, *Nanoscale*, 2017, DOI: 10.1039/C7NR01787A.

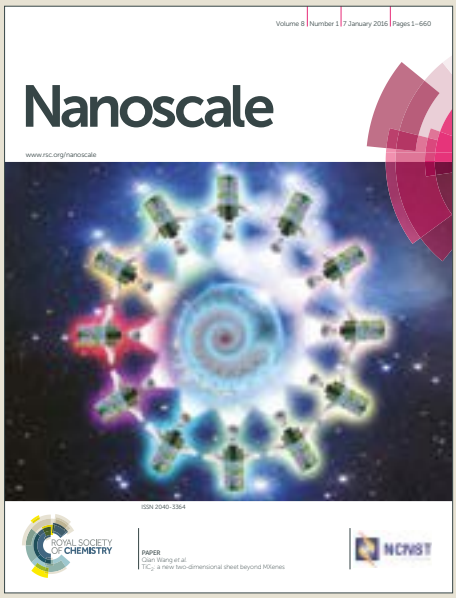

This is an Accepted Manuscript, which has been through the Royal Society of Chemistry peer review process and has been accepted for publication.

Accepted Manuscripts are published online shortly after acceptance, before technical editing, formatting and proof reading. Using this free service, authors can make their results available to the community, in citable form, before we publish the edited article. We will replace this Accepted Manuscript with the edited and formatted Advance Article as soon as it is available.

You can find more information about Accepted Manuscripts in the author guidelines.

Please note that technical editing may introduce minor changes to the text and/or graphics, which may alter content. The journal's standard Terms & Conditions and the ethical guidelines, outlined in our author and reviewer resource centre, still apply. In no event shall the Royal Society of Chemistry be held responsible for any errors or omissions in this Accepted Manuscript or any consequences arising from the use of any information it contains.

View Article Online
DOI: 10.1039/C7NR01787A

Journal Name

ARTICLE

ESIPT and FRET Probes for Monitoring Nanoparticle Polymer Coating Stability

Received 00th January 20xx,
Accepted 00th January 20xx

DOI: 10.1039/x0xx00000x

www.rsc.org/

Julio. C. Azcárate[a†], Sebastián A. Díaz[b†], Jonathan A. Fauerbach[c], Florencia Gillanders[b], Aldo A. Rubert[a], Elizabeth A. Jares-Erijman[c‡], Thomas M. Jovin[b], Mariano H. Fonticelli[a*]

Coating strategies of inorganic nanoparticles (NPs) can provide properties unavailable to the NP core alone, such as targeting, specific sensing, and increased biocompatibility. Non-covalent amphiphilic NP capping polymers function via hydrophobic interactions with surface ligands and are extensively used to transfer NPs to aqueous media. For applications of coated NPs as actuators (sensors, markers, or for drug delivery) in a complex environment, such as biological systems, it is important to achieve a deep understanding of the factors affecting coating stability and behavior. We have designed a system that tests the coating stability of amphiphilic polymers through a simple fluorescent readout using either polarity sensing ESIPT (excited state intramolecular proton transfer) dyes or NP FRET (Förster resonance energy transfer). The stability of the coating was determined in response to changes in polarity, pH and ionic strength in the medium. Using the ESIPT system we observed linear changes in signal up to ~20-25% v/v of co-solvent addition, constituting a break point. Based on such data, we propose a model for coating instability and the important adjustable parameters, such as the electrical charge distribution. FRET data provided confirmatory evidence for the model. The ESIPT dyes and FRET based methods represent new, simple tools for testing NP coating stability in complex environments.

Introduction

General strategies for transferring nanoparticles (NPs) from organic to aqueous media have successfully broadened their scope of application, in particular in the biomedical field. Phase transfers are usually undertaken according to three general strategies: 1) ligand exchange; 2) ligand adsorption; and 3) NP coating.[1–3] NP coating can in turn be subdivided into either inorganic coating, such as SiO_2 coating, and capping of organic ligands on the NP surface via an amphiphilic polymer. This last strategy has been extensively exploited with AuNPs, AgNPs, superparamagnetic iron oxide nanoparticles (SPIONs), and quantum dots (QDs), among many others.[4,5] However, further investigations and strategies are required to define factors destabilizing the NP coating, an issue poorly represented in the literature.[6,7]

Investigations of the stability of capping-modification strategies have mainly focused on the general colloidal stability of the NPs, and have relied on assessment of aggregation and/or biocompatibility.[1,8] It is crucial to differentiate between changes in stability due to NP interactions or to coating degradation. Within the context of cellular imaging or nanosensing, a NP probe may interact with multiple environments and moieties, including small molecules, proteins, membranes, the cytosol, and nuclear envelopes.[9] The necessity for understanding the underlying fundamental mechanisms as well as the capability to sense and quantify the stability of NP coats is an absolute requirement for predicting NP-probe interactions.[10] This dictum applies particularly to functionalized NPs carrying targeting moieties or drug payloads.[11]

The amphiphilic polymer prepared by modifying poly[isobutylene-*alt*-maleic anhydride] (PMA) -an alternating copolymer of succinic anhydride rings separated by butylene residues, with alkyl chains- was first proposed in 2004 by Parak and colleagues as a general strategy for NP solubilization[12] and has been applied in a broad range of systems and constructs.[13] An important advantage of PMA polymers is that they can be modified by very simple chemistry prior to or after NP coating. They have also been shown to exhibit long-term (> 1 year)

[a] Instituto de Investigaciones Fisicoquímicas Teóricas y Aplicadas (INIFTA), Facultad de Ciencias Exactas, Universidad Nacional de La Plata - CONICET Sucursal 4, Casilla de Correo 16, 1900 La Plata, Argentina.
[b] Laboratory of Cellular Dynamics, Max Planck Institute for Biophysical Chemistry, Am Fassberg 11, 37077, Göttingen, Germany.
[c] Departamento de Química Orgánica, Facultad de Ciencias Exactas y Naturales, Universidad de Buenos Aires, 1428 Buenos Aires, Argentina.
*Corresponding Author
e-mail mfonti@inifta.unlp.edu.ar (M.H.F.).
Web: http://nano.quimica.unlp.edu.ar;
Fax +54 221 425 4642; Ph +54 221 425 7430;
† J.C.A. and S.A.D. contributed equally to this work.
‡ E.A.J-E Deceased Sept.29, 2011.
SAD, Center for Bio/Molecular Science and Engineering, Code 6900, U.S. Naval Research Laboratory, Washington, DC, 20375, USA
JAF, Miltenyi Biotec GmbH, Friedrich-Ebert Str. 68, 51429 Bergisch-Gladbach, Germany
FG, Laboratorio de Investigación y Desarrollo, Akapol S.A., Buenos Aires.
Electronic Supplementary Information (ESI) available: Complementary information about details in purification methods, AcFE and AcFC spectra deconvolution, and spectra obtained by addition of other co-solvents on AuNP@PMA-FC dispersions. See DOI: 10.1039/x0xx00000x

View Article Online
DOI: 10.1039/C7NR01787A

colloidal stability. We therefore selected PMA coated gold NPs (AuNPs) and semiconductor nanocrystals, QDs, as the investigated models. Two strategies were utilized to determine and consequently understand the stability of the PMA coating on the hydrophobic NPs: 1) The integration of environmentally sensitive dyes within the PMA coated AuNPs, and 2) Förster Resonance Energy Transfer (FRET) determinations to estimate distance changes between the QD cores and their coatings.

The coating of NPs by amphiphilic polymers is based on the hydrophobic interactions of the alkyl chains of the polymer and the surface ligands of the NP. Therefore, it is reasonable to postulate that changes in polarity in this microenvironment may cause destabilization of the superficial coating. Our rationale is that polarity sensing dyes based on Excited State Intramolecular Proton Transfer (ESIPT), particularly the 3-hydroxychromone (3-HC) family, constitute unique fluorescent ratiometric reporters on hydrophobicity and hydrogen bonding, as shown with both biological[14,15] and NP systems.[16–18] The ratiometric signal of 3-HC reporters derives from their dual-band emission spectra reflecting emission from excited states isomers undergoing rapid intramolecular proton transfer. Thus, in order to study the coating stability we have covalently modified PMA-based polymers with 3-HC moieties, and we have used them to solubilize AuNPs. This lead to a nanoparticle-polymer assembly, AuNP-PMA-ESIPT, which can report on changes in ionic strength, solvation and/or pH. We found the AuNP-PMA-ESIPT system shows unprecedented sensitivity to small changes in medium composition. Additionally, the use of different ESIPT probes showed consensus on a maximum coating stability up to 20% of co-solvent addition. Indeed, further addition of co-solvent makes the polymer coating unstable, most likely leading to removal through what we have termed polymer stripping. In complementary determinations, we used FRET as an efficient reporter of changes in distances in the Å scale,[19] thereby confirming separation of the polymer coat from the NP under controlled conditions.

Experimental

Synthesis of fluorescent reporter molecules and conjugation to amphiphilic polymer for posterior NP Coating.

The two ESIPT probes based on 3-HC derivatives in position 2 with 4-(diethylamino)phenyl (FE) and 2-furanyl (FC), see scheme 1, and photocromic (PC) molecules were synthesized according to previously reported methodologies.[15,20] The ESIPT probes were synthesized as amine derivatives in position 6 allowing for nucleophilic attacks on the anhydride groups of the polymer forming a covalent amide bond. The preparation of the ESIPT containing amphiphilic polymer was as follows: 50 mg (8.33 µmoles polymer, 0.3 mmoles monomer) of PMA (Sigma-531278, MW ~6,000), 1.1 mg (3.33 µmoles) of 6-NH_2FE [2-[4-(diethylamino)phenyl]-3-hydroxy-4-oxo-6-amino-4H-chromen] and 0.5 ml of anhydrous THF were introduced into a dry 5 ml round-bottom flask. The mixture was sonicated for one min to dissolve and suspend all solids in solution, and was stirred at 60 °C overnight. A solution of 46.3 mg (25 mmoles) of dodecilamine and 1.7 mL of anhydrous THF were added and stirring was maintained for 6 h. The reaction was terminated by solvent evaporation and the modified polymer purified as previously reported[20] by size exclusion chromatography using Sephadex® LH-20 and $CHCl_3$ as stationary and mobile phases, respectively. The polymer obtained is referred to as PMA-1FE-75CN_{12}, given that it contained 1% of FE and 75% of dodecilamine with respect to the total number of monomer units. Similar conditions were used for 6-NH_2FC [6-amino-2-(2-furanyl)-3-hydroxy-4H-1-benzopyran-4-one] to obtain PMA-1FC-75CN_{12} polymer.

The preparation of the FRET competent amphiphilic polymer was as follows, 6 mg (1 µmole polymer, 40 µmoles monomer) of PMA were placed in a dry 10 mL round-bottom flask. A 1:1 DMF:DMSO solution containing 0.2 mg of Alexa647 cadaverine (0.16 µmole) was added. The solution was stirred at 60 ºC for 90 min and then 7.7 mg (14 µmoles) of PC [6-amino-N-(3-(3,3,4,4,5,5-hexafluoro-2-(2-methylbenzo[b]thiophen-3-yl)cyclopent-1-enyl)-2-methylbenzo[b]thiophen-6-yl)hexanamide] was added in the minimal possible volume of THF, typically 50-100 µl. Then, 1.85 mg (10 µmoles) of dodecylamine was added and the reaction stirred overnight at 60 ºC. An additional 3.7 mg (20 µmoles) of dodecylamine were added and allowed to react for another 6 h. The product was purified and characterized as previously described.[21]

AuNP Coating and purification

AuNPs were coated with the ESIPT modified amphiphilic polymers described above. The AuNPs protected by dodecanethiol were prepared with the biphasic Brust-Schiffrin method. The diameter of the AuNPs was regulated by the thiol to gold ratio.[22] The coatings were carried out at constant surface to polymer ratio (70 monomers per nm^2) for all of the AuNP diameters.[23] A solution of ESIPT- polymer in $CHCl_3$ was added to a solution of AuNPs in the same solvent. The mixture was stirred at 40 °C for 2 h, after which the solvent was slowly evaporated until complete dryness. 1× TBE (Tris/Borate/EDTA, pH 8.5) buffer was added in excess, and the mixture gently stirred overnight. The purification was based on 1% agarose gel-electrophoresis with 1× TBE buffer as electrolyte, applying 10V/cm.[23] Bands were revealed under UV light, and excised. The product was recovered from the gel by electro-elution into cellulose dialysis tube of MWCO 3.5 kDa (see supporting information for details about purification and characterization of samples and byproducts). The phase transfer of the NPs to an aqueous medium is evidence of the successful coating by the amphiphilic polymer as the original Surface ligands would not allow for water solubilization.

The NP FRET assay QDs were prepared by precipitation of 550 nm emitting QDs [CAN GmbH, Hamburg, Germany] from solvent supplied by the manufacturer and resuspended in $CHCl_3$. A solution of the FRET- polymer, also in $CHCl_3$, was added. The solutions were mixed in a round-bottom flask maintaining a proportion of 1 mg of polymer for every 900 pmol of QDs. The resulting solution was mixed at 65 °C for 2 h.

View Article Online
DOI: 10.1039/C7NR01787A

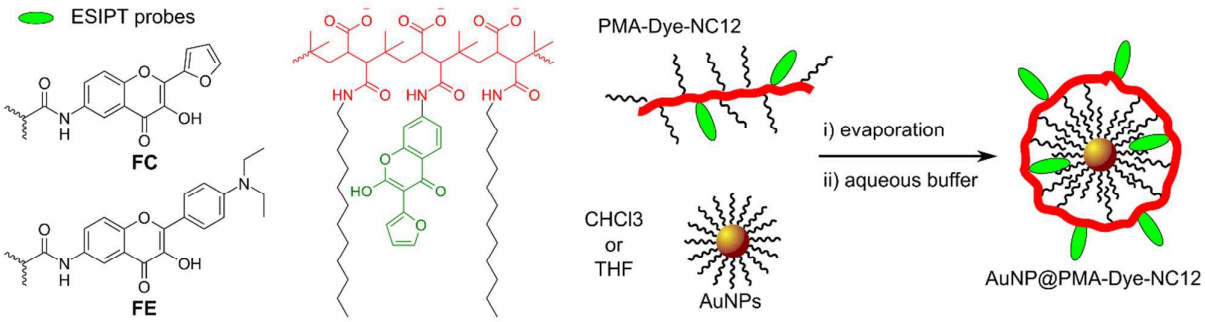

Scheme 1: Representation of the molecular structures of the FC and FE amide-derivatives. These flourophores were used as polarity and hydration probes coupled to the amphiphilic polymer backbone, represented by red wavy lines. On the right, a scheme of the functionalized amphiphilic polymer-AuNP assembly is presented.

The solvent was slowly evaporated until dryness followed by resupension in an excess of 50 mM SBB, pH 10. The samples were stirred mildly overnight at room temperature. Purification was performed by size exclusion chromatography as previously described.[21]

We note that there are different methods for purifying coated-NPs from the unassembled polymer (micelles or polymersomes), and it has been recently reported that ultracentrifugation has distinct advantages over the other techniques.[24,25] In this study we used agarose gel electrophoresis and size exclusion chromatography. Although small amounts of polymersomes may remain in the samples, their contribution to the fluorescence signal are insignificant. The characterization of purified samples and byproducts has demonstrated significant differences in the characteristics of coated-NPs and the unassembled polymer (see supporting information for more details).

Solvent-stability titrations

The titrations were realized using 100 μL of sample (A_{520} < 0.2) in microcuvettes followed by serial additions of organic solvents: isopropanol (*i*-PrOH), acetonitrile (MeCN), ethanol (EtOH) or tetrahydofuran (THF). After each addition the sample was mixed by pipetting up and down and the spectra were recorded after the sample had settled after 20 s. Absorbance spectra (300–800 nm) were also acquired on an UV–Vis Cary spectrophotometer utilizing a 10 mm optical path. The corresponding solvent spectrum (sample free) was utilized as a blank. Fluorescence spectra were acquired in parallel at 20 °C, with excitation wavelengths of 420 nm and 360 nm for FE and FC dyes, respectively, and 400 nm for QDs; 5 nm slits were used for both excitation and emission.

Results and discussion

The focus of the study was to design and implement a methodology to test the stability and behavior of PMA-coated NP sensors exposed to different environmental conditions of polarity, hydrogen bonding, basicity, pH and ionic strength.

We started by analyzing the effects of changes in polarity and hydrogen bonding reorganization on the stability of AuNP-PMA suspended in water. These were performed by titration assays in which a series of organic solvents (*i.e. i*-PrOH) were successively added to the NPs solutions. After each addition, changes were reported by modifications in the fluorescence spectra of the polarity-sensitive dyes covalently attached to PMA (i.e. FE, FC) surrounding AuNPs. The intensity ratio of the bands represented a direct measurement of the polarity in the microenvironment of the dye. Thus, the ratiometric fluorescent probes were capable of sensing changes of polarity, reflecting changes in coating structure and stability. Control assays conducted with free dye, free polymer, immiscible solvents and dilution experiments (see below) allowed us to properly interpret the results based on the latest ESIPT understanding. In parallel, we also monitored changes in FRET between PC and QDs in similar assemblies and conditions under which the fluorescent probes were independent of polarity and hydration. The FRET measurements provided direct evidence of polymer disassembling.

Lastly, for a deeper understanding of the early stage evolution of the assemblies as a consequence of their exposure to different environments, we tested the effects of changes in other variables such as pH, concentration and ionic strength.

Free ESIPT probes

The ESIPT probes have been widely used to sense medium polarity of neat solvents, mixtures of solvents, and also of protein misfolding and aggregation[15] and peptide interactions.[26,27] Hydration sensitivity has been widely reported for free probes[28,29] and after integration into micelles.[30] As a reference of free probes in solution, we used the acetyl derivative of FE and FC (denoted AcFE and AcFC, see

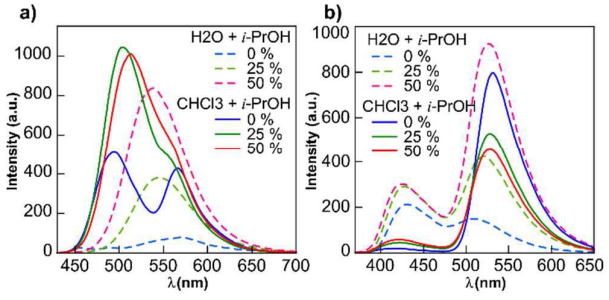

Figure 1: Fluorescence spectra of a) AcFE and b) AcFC probes in water (dashed lines) and chloroform (filled lines) with the indicated % v/v i-PrOH addition.

View Article Online
DOI: 10.1039/C7NR01787A

Scheme 1) in order to mimic the amide bond in position 6. AcFE and AcFC allowed us to test the behavior of the probe itself without the influence of the coating polymer and the NP in a wide range of solvent mixtures of water or chloroform (as an example of low polarity medium) with fractional additions of isopropanol from 0 to 50%v/v. This provided a baseline control for the probe fluorescence under the various conditions that were tested.

Figure 1 shows a summary of the AcFE and AcFC emission spectra in the different solvent mixes. The presence of an ESIPT equilibrium resulted in multiple fluorescence emission bands. In the case of the AcFE emission spectra, there were two well-resolved bands in 100% chloroform (Fig 1a, filled line). However, addition of *i*-PrOH collapsed the bands, diminishing the resolution between the peaks, resulting in a shoulder. In pure water AcFE did not show indications of ESIPT (Figure 1a, dashed line). Additionally AcFE was almost entirely quenched in water; addition of *i*-PrOH increased its total fluorescence intensity without resolving its emission bands (ESIPT may also be abrogated in this conditions). In contrast AcFC displayed a well-resolved dual emission spectra under all solvent combinations (Figure 1b). It is noticeable that the positions and relative intensities of the bands were highly dependent on the polarity of the environment, as well as the hydrogen bonding sensed by the dye. For both probes the shorter wavelength corresponds to the emission of the normal excited state (N*), while the longer-wavelength band originates from the tautomer (T*, ESIPT product) excited state.[31] An increase in media polarity or H-bonding led to a higher relative change in the intensity of the N* compared to the T* band. In protic polar solvents, an intermolecular hydrogen bond between the oxygen of the carbonyl group of the dye and the proton of the OH groups of the chosen solvents can be formed. When this occurs, the dye exhibits an emission band that is referred to as the H-bonded form H-N*. This third additional band H-N*, usually located between N* and T*, is not always well resolved.[32] Thus, peak positions and intensities are better determined by proper spectral deconvolution.[29] For AcFE the position of the H-N* in protonated organic solvents (like alcohols) is ~517 nm. On the other hand, in aqueous solutions, in which the ESIPT reaction is not significant, it is located at ~550 nm[33] (a complete set of spectral deconvolutions is available in the SI). When the N* and H-N* bands cannot be resolved, the low wavelength emission band is broader and exhibits an overall bathochromic shift. Both AcFE and AcFC had a very low photoluminescence quantum yield (PLQY) in water;[34] the addition of *i*-PrOH strongly increased the fluorescense signal.[15,35]

Comparison of free probes and NP constructs

The emission spectra of FE and FC in polymer coated NPs compared with those of the free ESIPT probes indicate a bathochromic shift, particularly in the T* band (**Error! Reference source not found.**2).

The FE probes (Figure 2a) of the AuNP polymer constructs showed a similar I_{N*}/I_{T*} ratio as in $CHCl_3$, a low polarity medium. However, the two emission bands were broader than for AcFE in $CHCl_3$. These two findings are somewhat contradictory, leading to speculations regarding the structure of the polymer, in particular different probe positions and/or orientations in the inner and outer hydrophobic shells.[16] In the case of the FC probes within the NP constructs, the T* band was red shifted 44 nm with respect to the free AcFC probe in water, indicating that the probe in the constructs was not in direct contact with bulk water (Figure 2). As with the FE probe the location of the T* band for the FC probe in coated NPs was closer to that in $CHCl_3$ than in water, although the ratio for FC probes in the polymer coated NPs did not correlate with either a pure water or $CHCl_3$ environment. It is notable that in the fluorescence spectra with 25% added *i*-PrOH, a shoulder was observed at a wavelength similar to that of AcFC T* band in $CHCl_3$. We conclude that under this condition a small number of FC molecules were located deep inside the hydrophobic shell with a significant fraction in the hydrophobic region near the polymer surface interface. The latter molecules would present a spectral emission similar to that in $CHCl_3$, but with a decreased T* band due to interaction and consequent quenching by water molecules present in the Stern layer. It is important to note that the fluorescence emission spectra will be dominated by molecules with higher PLQY. The proposed model of dye distribution is consistent with publications suggesting that ESIPT dyes can be located within the hydrophobic shell or in the Stern layer.[16] The strong red shift could thus be attributed to the influence of the electric field changes in the Stern layer.[30,36] Indeed, if only subtle changes in the structure of the assemblies occur, the probes in the hydrophobic region would not be altered significantly. In contrast, the fluorophores in the Stern layer should sense even subtle alterations in polarity, electric field, or hydrogen bond formation.

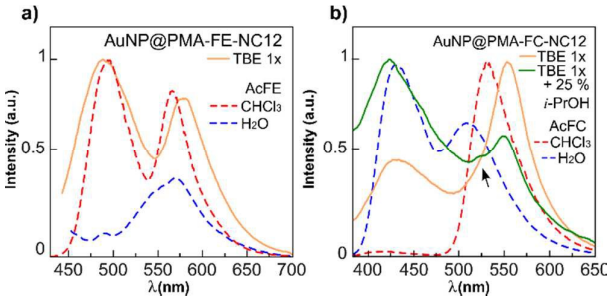

Figure 2: Comparison of ESIPT probes within NP constructs and free in solution. a) FE b) FC.

Co-solvent Addition / Media Polarity

The ESIPT response provides insight into the structure and stability of the assemblies when they are exposed to different media. First, it is important to stress that the polymer self-assembles on the NP due to the preferential interaction with the NP surface ligands. Thus, the phase transfer of the NPs was realized by adding aqueous buffer to fully dried NP/polymer mixtures. On the other hand, the polymer does not coat the NPs in purely non-polar solvents (THF, $CHCl_3$).[37] For this

View Article Online
DOI: 10.1039/C7NR01787A

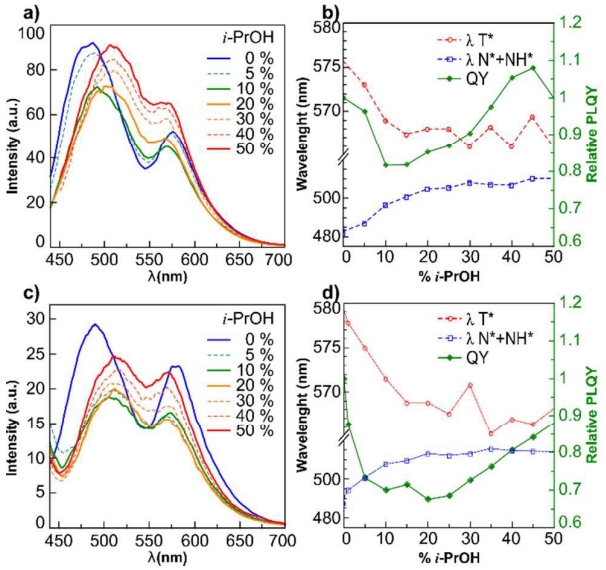

Figure 3: Emission spectra of 2 nm (a) and 4 nm (c) AuNP@PMA-FE as i-PrOH % increased. Band shifts and PLQY relative to 0% i-PrOH are shown in (b) and (d) for 2 nm and 4 nm, respectively.

reason, it was of interest to investigate the outcome of adding miscible organic solvents to aqueous NP solutions.

First, tests with immiscible solvents ($CHCl_3$) and dilution as controls were realized. It was observed that upon $CHCl_3$ addition the coated-NPs remained very stable in the aqueous phase unless harsh conditions such as high acidity (pH 1) and sonication were applied.[37] This result is explained by considering that the polymer's carboxyl groups favorably interact with aqueous solutions. Addition of $CHCl_3$ did not measurably change the fluorescence spectra nor (in other experiments) the relative fluorescence intensities. These measurements also served as controls for the purification of the samples; unbound polymer would show considerable affinity for the non-polar medium ($CHCl_3$) and demonstrated considerable changes in the ESIPT fluorescence.

We then proceeded to study miscible co-solvents, both protic (EtOH, *i*-PrOH) and aprotic (MeCN, THF) as a way of changing media polarity. It is important to note that the placement of the dyes is primarily within the hydrophobic environment established between the NP surface and the polymer coating.[16] While the media is characterized by macroscopic properties, the ESIPT dyes can exist in, and report on different microenvironments (See Scheme 1). Figure 3 shows the emission spectra of AuNPs coated with PMA-1FE-75CN_{12} (AuNPs@PMA-1FE-75CN_{12}) suspended in 1× TBE after consecutive additions of *i*-PrOH (from 0 to 50%v/v). At 0% i-PrOH the FE dye shows two bands located at 475 nm and 580 nm. The analysis of this spectrum is consistent with the idea that the FE is mainly surrounded by the hydrophobic chains of the polymer. Indeed, this two-band spectrum is completely different from that of the free AcFE in water or protic media. Addition of *i*-PrOH from 0 to 10% produced a reduction in the photoluminescence quantum yield (PLQY, as full integration under the curve) accompanied by bathochromic and hypsochromic shifts of the N* and T* band, respectively (N* band: 475→500 nm, T* band: 580→550 nm). Similar trends in band shifts - but of lower magnitudes - were observed between 10 to 20% of *i*-PrOH, and a slightly increased PLQY was also evident in these solvent ranges (see green curves in Figure 3b,d). Finally, at 50% of *i*-PrOH the N* and T* bands reached positions centered at 525 nm and 545 nm, respectively. The initial decrease in PLQY was due to the greater interaction of the probe with water molecules (the cosolvent decreases the hydrophobicity of the NP-polymer microenvironment) and subsequently increased due to further interaction with *i*-PrOH molecules. Although the PLQY fluctuated the final values were similar to or slightly below the initial levels. The wavelength shifts are most likely due to an increased fraction of the H-N* component, a behavior clearly shown by the free probe (Fig. 1, and SI). Similar behaviors were observed both for 2 nm and 4 nm AuNPs (Figure 3). However, the FE probe showed a greater I_{N*}/I_{T*} ratio when coated on 2 nm AuNPs as compared to 4 nm AuNPs. The 2 nm AuNPs have higher curvature and their hydrophobic assembly would be more heterogeneous, resulting in a larger proportion of FE units exposed to the external environment.[1] When the co-solvent is added in small quantities it induces changes in the assembly that increase the interaction of FE with water. For the higher *i*-PrOH amounts (*i*-PrOH content > 20%v/v), we observed a complex behavior, hypothesized as a detachment of polymer chains from the assembly. The NP-FRET assays (see corresponding section) provided supporting evidence for polymer stripping.

Because the H-N* band was absent in the FC spectra the comparison between protic and aprotic solvents was simpler with this probe. Thus, we also studied AuNPs coated with polymers containing FC. Figure 4 shows the FC spectra for increasing *i*-PrOH amounts, and the band intensity ratio (I_{N*}/I_{T*}) after adding *i*-PrOH and MeCN (results for other solvents are shown in the SI). In all cases, an increase in the N* band intensity was observed. The intensity at lower wavelengths also increased due to scattering. The plot of I_{N*}/I_{T*} ratio vs. *i*-PrOH content shows an almost linear increase up to 20% co-solvent, indicating that the FC experienced – on average - a more polar environment as the co-solvent was added. This result was counterintuitive inasmuch as the dielectric constant (or polarity) of the bulk solution was

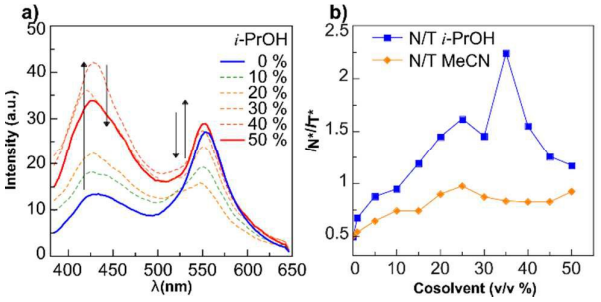

Figure 4: (a) Spectral changes of 2 nm AuNP@PMA-FC-75CN12 as i-PrOH % increased; (b) IN*/IT* traces for i-PrOH (blue) and MeCN (orange) co-solvent addition. See SI for spectra and band ratios for the other solvents.

View Article Online
DOI: 10.1039/C7NR01787A

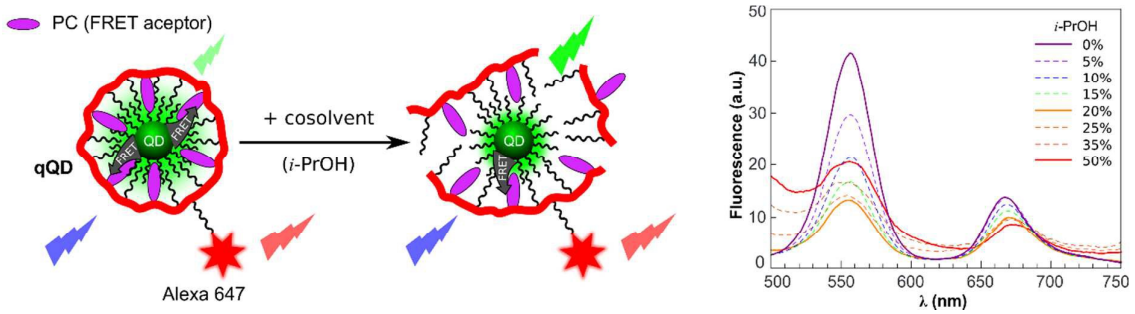

Scheme 2: Representation of quenched QDs (qQDs) assembly structures and their changes (polymer stripping) after co-solvent addition. On the right side, the fluorescence spectra as a function of i-PrOH %.

progressively diminished. This is the crucial experimental find and we rationalize the experimental result by invoking an increased interaction of FC with water as a consequence of polymer-conformational changes, leading to a blurring of the interface between the exterior (aqueous) and interior (hydrophobic) compartments. That is, the dyes no longer sense the pre-existing equilibrium between the hydrophobic microenvironment and the bulk solution, but rather a progressive decrease in stability. It is noteworthy that the break in monotonous increment of the I_{N*}/I_{T*} ratio occurred at the same point (about 20-25 % *i*-PrOH) for AuNPs coated with either ESIPT polymer. The erratic behavior at higher co-solvent addition (Figure 4b) suggested abrupt changes in dye environment, which may again reflect polymer stripping and formation of secondary polymer structures. An additonal strategy was adopted to confirm the hypothesis.

NP FRET assays

To confirm the existence of polymer stripping, we performed distance measurements using QDs, which emit at 550 nm, coated with a polymer containing a quenching molecule (PC) and a secondary emitting molecule (Alexa647).[21] The Förster radius with the QD donor was 4.1 nm for both dyes, but the PC is located 3.1±0.1 nm and the Alexa647 6.0±0.4 nm from the QD surface.[21] Thus the PC acted as a strong FRET acceptor diminishing the QD emission due to its closer placement (Scheme 2) and greater number (6 PC per QD) as compared to the Alexa647 (1 dye per QD).[38] FRET transfers energy through the interaction of the donor and acceptor dipoles, the efficiency of the transfer being inversely proportional to the sixth power of the donor-acceptor distance. Therefore, the QD emission increases with greater PC distances or a decrease in the number of PC acceptors bound to the QD. The Alexa647 served principally as an internal fluorescent standard of colloidal stability.[21] Progressive polymer stripping from the central core constitutes a dramatic change in the core-polymer distance and abrogation of FRET, as was experimentally observed.

A solution of quenched QDs (qQDs) was titrated with up to 50% *i*-PrOH or MeCN in the same manner as for the AuNPs described in the previous section. Control experiments were conducted by titrating the QDs with SBB buffer solution and $CHCl_3$, as well as performing the same assays on QDs coated with unmodified amphiphilic polymer containing only alkyl chains (no dyes). Neither $CHCl_3$ nor dilution with buffer altered the fluorescence ratio of qQDs. Thus, as expected, the addition of these two solvents did not observably affect the polymer/QD interaction, indicating that any changes observed in fluorescence and absorbance spectra after addition of *i*-PrOH and MeCN are due to structural rearrangements of the amphiphilic polymer coating.

Figure 5a shows the absorbance values of dispersions that contained the qQD at different *i*-PrOH %. Particular wavelengths can be used to observe the individual components: the quencher molecule (PC; 395 nm), the internal standard (Alexa647; 650 nm) and the QD cores (540 nm). The absorbance traces remained fairly steady from 0% *i*-PrOH up to 20% *i*-PrOH, after which the 395 nm absorbance of the PC increases significantly reaching a plateau at 35% *i*-PrOH, where the Alexa647 absorbance decreases continuously. The increase of the 395 nm absorbance had a strong contribution from a scattering signal, while the change in bulk solvent polarity slightly decreased the Alexa647 absorption.[39] The increase in scattering is additional evidence in support of the polymer stripping hypothesis.

As seen in Figure 5b the titration with miscible co-solvents affected the QD polymer coat stability. We represent the titrations as the fluorescence intensity of the QDs as a function of the added co-solvent volume fraction. The PLQY of the control QDs (PMA coated QDs with no dyes) decreased slowly up to 20%, and then abruptly dropped from 20-30% and then re-stabilized. In contrast, the emission of the qQDs with both *i*-PrOH and MeCN, corrected for dilution and scattering,

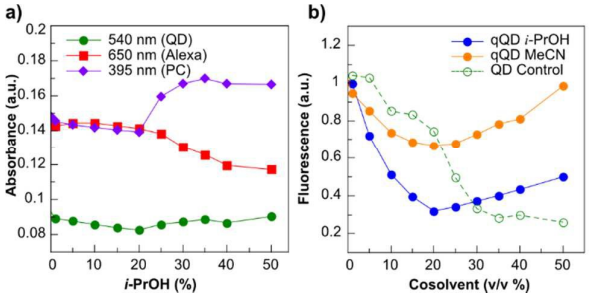

Figure 5: Absorbance (a) and emission (b) of qQDs as a function of % co-solvent. The fluorescence was normalized to 0% co-solvent, and corrected for dilution and scattering.

View Article Online
DOI: 10.1039/C7NR01787A

decreased rapidly but then increased starting at 20% v/v co-solvent. The Alexa647 emission decreased slowly throughout the titration in line with the decrease in extinction coefficient, attesting to the colloidal stability of the solution.

Since both the control QDs and the qQDs showed a lower PLQY for 0-20% co-solvent, interpretation of the data in that range presented a challenge. FRET is only slightly affected by properties (refractive index) of the transfer medium and estimation of the QD-PC distance is ambiguous due to the changes in PLQY of the control QD.[40] However, it is significant that at the same breaking point observed in the ESIPT polymers, i.e. at ~20% co-solvent, the qQD intensity began to increase. At 50% v/v of both co-solvents the fluorescence of the qQDs was ~20% greater than the values of the respective minima (all values corrected for dilution and scattering), while in the control experiments the QD PLQY was stable for *i*-PrOH content >30%. Thus, the fluorescence enhancement can be attributed to a lower FRET efficiency, due either to a decrease in the number of acceptors or to an increase in the average distance from 3.1 to 4.2 nm.[37] Most likely a combination of these factors was involved: some polymer strands were directly removed and the remaining strands were attached more "loosely", allowing for a greater distance between the quencher and QD surface.

We conclude that FRET served to corroborate and complement the ESIPT data observing the destabilization of the polymer coat at 20% v/v of miscible co-solvent addition. The addition of co-solvents decreased the medium polarity and consequently the stability of the NP coating caused by the preferential hydrophobic interactions of the NP-polymer nanoenvironment in response to a polar bulk solution.

pH, Dilution and ionic strength

As a general test of the other parameters of coating stability the addition of *i*-PrOH was selected as it showed the greatest changes and largest linear range. Addition of a co-solvent not only modified the medium's overall polarity but also its dielectric constant, pH, and ionic strength. It can be anticipated that these changes could alter the stability of the coated NP by inducing variations on their overall superficial charge. In this regard, it is important to note that the ESIPT probes are sensitive to the local electric field.[36]

To test the influence of pH, we gradually acidified an AuNP@PMA-FE-NC$_{12}$ solution from pH 8.54 to a physiological value (pH 7.41). The total fluorescence intensity of the FE probe slightly decreased but without any shift of the band locations. The T* band was more sensitive to these changes, which can be interpreted as a greater interaction with H_2O molecules (Figure 6). Lowering the pH leads to a progressive protonation (neutralization) of the polymer-attached carboxylic groups. This modification in surface charge density appears to have increased the mobility of associated water molecules. Still lower pHs were not tested due to destabilization of the colloidal system (NP precipitation), which was manifested as an increase in the scattering signal observed at λ<450 nm. Addition of *i*-PrOH at the lower pH of 7.4 showed a significant increase in PLQY, with spectral shifts close to those observed in TBE buffer (See Figure 3C). Such behavior is consistent with the model presented in the literature for ESIPT dyes within micelles[30] and lipid bilayers,[32,33,41,42] in which it is proposed that the dyes are located within the internal hydrophobic layer but feel the effects of the Stern layer (*i.e.* an inner electrically charged zone; see discussion above).

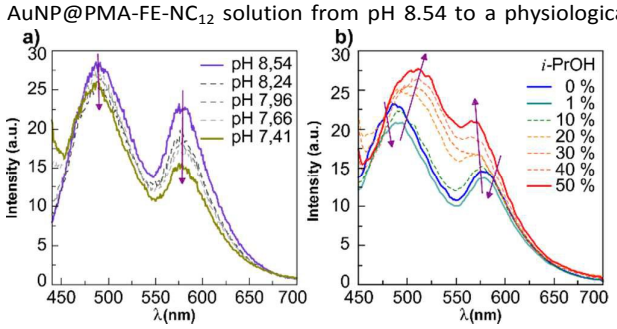

Figure 6: pH dependence of AuNP@PMA-FE-NC12 emission. a) Decrease in pH; b) polarity response at pH 7.4. (These plots correspond to 4 nm AuNPs)

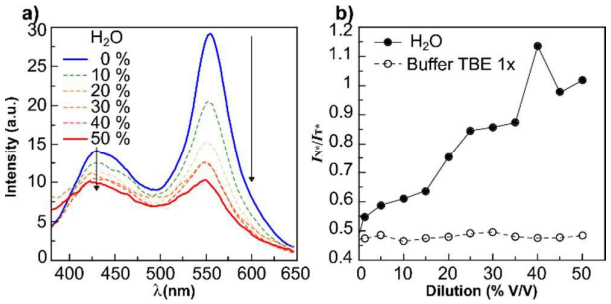

Figure 7: Effects of dilution by water (a, b) or buffer (b) on fluorescence spectra and IN*/IT* ratio of AuNP@PMA-FE-NC12.

The addition of a co-solvent to an aqueous solution containing coated NPs leads not only to changes in polarity. Dilution reduces the ionic strength, inducing another alteration in the structure of polymer coated NPs. To uncouple these effects from those due to polarity, dilution assays with water and buffer solution (1×TBE) were performed, and the fluorescence spectra were recorded (Figure 7). The I_{N^*}/I_{T^*} ratio showed (panel b) that dilution with water modified the local environment sensed by the dye, yet no changes were observed upon addition of buffer. The amphiphilic polymer presents a large surface charge which is partially balanced by counterions in the Stern layer. Modifying the ionic strength of the bulk solution results in observable changes at the NP surface, as revealed by the ESIPT dyes (previous section). This is in good agreement with the results shown previously in the pH dependency experiments as well as upon co-solvent addition.

Conclusions

In this study we demonstrated that polarity probes from the family of 3-HC are useful reporters to evaluate the stability of amphiphilic coatings. An ESIPT-based sensing system can be assembled easily using AuNP, PMA and dodecylamine. The fluorescent probes not only are sensitive to changes in

View Article Online
DOI: 10.1039/C7NR01787A

polarity, but also to variations of the local electric field. Thus, the ESIPT probes can report on changes in ionic strength, solvation and/or pH (of greater relevance to biological systems). The AuNP-PMA-ESIPT system has shown unprecedented sensitivity to small changes, e.g. as low as 2%, in the total medium composition. Additionally, the use of different ESIPT probes (FC and FE derivatives) showed consensus on a maximum coating stability up to 20% of *i*-PrOH addition, although it is possible that different ESIPT probes can be more attuned or better suited to different assays or constructs. Together, the results achieved with ESIPT probes indicate that the nature of the interactions and solvent structure play an important role in ion distribution and water mobility at the interface (Stern layer) between polymer coated NPs and aqueous medium.[43] These in turn modify the equilibrium between the hydrophobic nanoenvironment of the polymer coated NP and the rest of the aqueous bulk buffer solution. Indeed, after further addition of this co-solvent the polymer coating becomes unstable, most likely undergoing a stripping process. Stripping above 20-25% of *i*-PrOH is not solely due to changes in polarity, but also in ionic strength and variations of the charge distribution in the interfacial region.

The polymer stripping model derived from ESIPT measurements was further verified by complementary FRET measurements on a similar system using QDs coated with a FRET competent polymer. The FRET studies not only demonstrated the ability of solvents to separate the coating from NPs, but also provided a quantitative measurement of the process and related threshold limits. This result is relevant inasmuch as NPs are often touted as drug-delivery mechanisms and multi-component solvents are often utilized in pharmaceuticals as well as in cosmetic preparations. Although complex biological environment and cell membranes are quite different from binary mixtures of H_2O and co-solvents, further studies must be carried out to determine the fates of the polymer coated NPs when used in non-optimized contexts.

We envision that the detailed strategies described here could be applied to a variety of NP systems and (amphiphilic) coating combinations. Ongoing research is focused on the development and characterization of new surface ligands, optimal ligand densities, and derivitization of the NP surfaces.[44] ESIPT modified polymers may be useful reporters of the stability of NPs coated with various surface ligands. Inversely different polymer modifications, such as longer/shorter hydrophobic chains or different attachment groups can also be reported by ESIPT dyes. Additionally, the ESIPT dyes may be able to report on similar structural changes within polymersomes, micelles, or other amphiphilic nanostructures. Traditional methodologies for observing changes in amphiphilic nanostructures either require multiple setups for surface tension, viscosity, and conductance measurements or the detection of dye partitioning;[45] in the case of multi-component compact structures such as coated NPs these options become complex. The methods demonstrated in this article present a valid alternative, with an easy and continuous monitoring setup that can be realized on a simple fluorimeter. Moreover, the strategy is independent of NP concentration due to the ratiometric aspect of the signal. As the system is quite sensitive and utilizes multiple fluorescent dyes per NP (counteracting photobleaching), its use in cellular microscopy for determining local environmental conditions can be anticipated.

Acknowledgements

Elizabeth A. Jares-Erijman passed away while this research was being carried out. The surviving authors dedicate this publication to her memory and in acknowledgment of her inspiration, leadership, contributions, and outstanding personal qualities. The authors thank to Dr. Andrey S. Klymchenko and Dr. Guillermo Menendez for helpful discussion.

This work was supported by CONICET (PIP 0333), UNLP and "Agencia Nacional de Promoción Científica y Tecnológica" (PRH-74).

References

1 R. A. Sperling and W. J. Parak, *Philos. Trans. A. Math. Phys. Eng. Sci.*, 2010, **368**, 1333–1383.
2 Z. Ali, A. Z. Abbasi, F. Zhang, P. Arosio, A. Lascialfari, M. F. Casula, A. Wenk, W. Kreyling, R. Plapper, M. Seidel, R. Niessner, J. Knöll, A. Seubert and W. J. Parak, *Anal. Chem.*, 2011, **83**, 2877–2882.
3 M. G. Soliman, B. Pelaz, W. J. Parak and P. del Pino, *Chem. Mater.*, 2015, **27**, 990–997.
4 D. Jańczewski, N. Tomczak, M.-Y. Han and G. J. Vancso, *Nat. Protoc.*, 2011, **6**, 1546–1553.
5 S. A. Díaz, F. Gillanders, K. Susumu, E. Oh, I. L. Medintz and T. M. Jovin, *Chem. - A Eur. J.*, 2017, **23**, 263–267.
6 G. Palui, F. Aldeek, W. Wang and H. Mattoussi, *Chem. Soc. Rev.*, 2014, **44**, 193–227.
7 N. Zhan, G. Palui and H. Mattoussi, *Nat. Protoc.*, 2015, **10**, 859–874.
8 G. Charron, D. Hühn, A. Perrier, L. Cordier, C. J. Pickett, T. Nann and W. J. Parak, *Langmuir*, 2012, **28**, 15141–15149.
9 F. Zhang, E. Lees, F. Amin, P. RiveraGil, F. Yang, P. Mulvaney and W. J. Parak, *Small*, 2011, **7**, 3113–3127.
10 W. G. Kreyling, A. M. Abdelmonem, Z. Ali, F. Alves, M. Geiser, N. Haberl, R. Hartmann, S. Hirn, D. J. de Aberasturi, K. Kantner, G. Khadem-Saba, J.-M. Montenegro, J. Rejman, T. Rojo, I. R. de Larramendi, R. Ufartes, A. Wenk and W. J. Parak, *Nat. Nanotechnol.*, 2015, **10**, 619–623.
11 C. Hoskins, P. K. Thoo-Lin and W. P. Cheng, *Ther. Deliv.*, 2012, **3**, 59–79.
12 T. Pellegrino, L. Manna, S. Kudera, T. Liedl, D. Koktysh, A. L. Rogach, S. Keller, J. Rädler, G. Natile and W. J. Parak, *Nano Lett.*, 2004, **4**, 703–707.
13 D. Jańczewski, N. Tomczak, Y. W. Khin, M.-Y. Han and G. Julius Vancso, *Eur. Polym. J.*, 2009, **45**, 3–9.
14 J. A. Fauerbach, D. A. Yushchenko, S. H. Shahmoradian, W. Chiu, T. M. Jovin and E. A. Jares-Erijman, *Biophys. J.*, 2012, **102**, 1127–1136.
15 D. A. Yushchenko, J. A. Fauerbach, S. Thirunavukkuarasu, E. A. Jares-Erijman and T. M. Jovin, *J. Am. Chem. Soc.*, 2010, **132**, 7860–7861.
16 F. Amin, D. A. Yushchenko, J. M. Montenegro and W. J. Parak, *ChemPhysChem*, 2012, **13**, 1030–1035.

View Article Online
DOI: 10.1039/C7NR01787A

17 Y. D. Álvarez, J. A. Fauerbach, J. V. Pellegrotti, T. M. Jovin, E. A. Jares-Erijman and F. D. Stefani, *Nano Lett.*, 2013, **13**, 6156–6163.
18 E. M. N. Oliveira, F. L. Coelho, M. L. Zanini, R. M. Papaléo and L. F. Campo, *ChemPhysChem*, 2016, **98**, 1257–1261.
19 I. Medintz and N. Hildebrandt, Eds., *FRET - Förster Resonance Energy Transfer: From Theory to Applications*, John Wiley & Sons, 2013.
20 S. A. Díaz, G. O. Menéndez, M. H. Etchehon, L. Giordano, T. M. Jovin and E. A. Jares-Erijman, *ACS Nano*, 2011, **5**, 2795–2805.
21 S. A. Díaz, L. Giordano, T. M. Jovin and E. A. Jares-Erijman, *Nano Lett.*, 2012, **12**, 3537–3544.
22 M. J. Hostetler, J. E. Wingate, C.-J. Zhong, J. E. Harris, R. W. Vachet, M. R. Clark, J. D. Londono, S. J. Green, J. J. Stokes, G. D. Wignall, G. L. Glish, M. D. Porter, N. D. Evans and R. W. Murray, *Langmuir*, 1998, **14**, 17–30.
23 M. T. Fernandez-Argüelles, A. Yakovlev, R. A. Sperling, C. Luccardini, S. Gaillard, A. S. Medel, J.-M. Mallet, J.-C. Brochon, A. Feltz, M. Oheim, W. J. Parak, M. T. Fernández-Argüelles and A. Sanz Medel, *Nano Lett.*, 2007, **7**, 2613–7.
24 J. Hühn, C. Carrillo-Carrion, M. G. Soliman, C. Pfeiffer, D. Valdeperez, A. Masood, I. Chakraborty, L. Zhu, M. Gallego, Z. Yue, M. Carril, N. Feliu, A. Escudero, A. M. Alkilany, B. Pelaz, P. del Pino and W. J. Parak, *Chem. Mater.*, 2017, **29**, 399–461.
25 P. Del Pino, F. Yang, B. Pelaz, Q. Zhang, K. Kantner, R. Hartmann, N. Martinez De Baroja, M. Gallego, M. Möller, B. B. Manshian, S. J. Soenen, R. Riedel, N. Hampp and W. J. Parak, *Angew. Chemie - Int. Ed.*, 2016, **55**, 5483–5487.
26 O. M. Zamotaiev, V. Y. Postupalenko, V. V. Shvadchak, V. G. Pivovarenko, A. S. Klymchenko and Y. Mély, *Bioconjug. Chem.*, 2011, **22**, 101–107.
27 V. V. Shvadchak, L. J. Falomir-Lockhart, D. A. Yushchenko and T. M. Jovin, *J. Biol. Chem.*, 2011, **286**, 13023–13032.
28 A. S. Klymchenko and A. P. Demchenko, *New J. Chem.*, 2004, **28**, 687.
29 W. Caarls, M. Soledad Celej, A. P. Demchenko and T. M. Jovin, *J. Fluoresc.*, 2010, **20**, 181–90.
30 R. Das, G. Duportail, L. Richert, A. Klymchenko and Y. Mély, *Langmuir*, 2012, **28**, 7147–7159.
31 V. V. Shynkar, A. S. Klymchenko, E. Piémont, A. P. Demchenko and Y. Mély, *J. Phys. Chem. A*, 2004, **108**, 8151–8159.
32 A. S. Klymchenko, G. Duportail, A. P. Demchenko and Y. Mély, *Biophys. J.*, 2004, **86**, 2929–2941.
33 V. Y. Postupalenko, V. V. Shvadchak, G. Duportail, V. G. Pivovarenko, A. S. Klymchenko and Y. Mély, *Biochim. Biophys. Acta - Biomembr.*, 2011, **1808**, 424–432.
34 A. S. Klymchenko, G. Duportail, T. Ozturk, V. G. Pivovarenko, Y. Mély and A. P. Demchenko, *Chem. Biol.*, 2002, **9**, 1199–1208.
35 A. S. Klymchenko, V. G. Pivovarenko and A. P. Demchenko, *J. Phys. Chem. A*, 2003, **107**, 4211–4216.
36 A. S. Klymchenko and A. P. Demchenko, *J. Am. Chem. Soc.*, 2002, **124**, 12372–12379.
37 S. a. Díaz, F. Gillanders, E. a. Jares-Erijman and T. M. Jovin, *Nat. Commun.*, 2015, **6**, 6036.
38 N. Hildebrandt, C. M. Spillmann, W. R. Algar, T. Pons, M. H. Stewart, E. Oh, K. Susumu, S. A. Díaz, J. B. Delehanty and I. L. Medintz, *Chem. Rev.*, 2017, **117**, 536–711.
39 S. E. Sheppard, P. T. Newsome and H. R. Brigham, *J. Am. Chem. Soc.*, 1942, **64**, 2923–2937.
40 E. A. Jares-Erijman and T. M. Jovin, *Nat. Biotechnol.*, 2003, **21**, 1387–95.
41 G. M'Baye, A. S. Klymchenko, D. a Yushchenko, V. V Shvadchak, T. Ozturk, Y. Mély and G. Duportail, *Photochem. Photobiol. Sci.*, 2007, **6**, 71–6.
42 A. P. Demchenko, Y. Mély, G. Duportail and A. S. Klymchenko, *Biophys. J.*, 2009, **96**, 3461–70.
43 R. Buchner, C. Baar, P. Fernandez, S. Schrödle and W. Kunz, *J. Mol. Liq.*, 2005, **118**, 179–187.
44 A. M. Smith, K. A. Johnston, S. E. Crawford, L. E. Marbella and J. E. Millstone, *Analyst*, 2017, **142**, 11–29.
45 O. K. Nag, J. Naciri, E. Oh, C. M. Spillmann and J. B. Delehanty, *Bioconjug. Chem.*, 2016, **27**, 982–993.